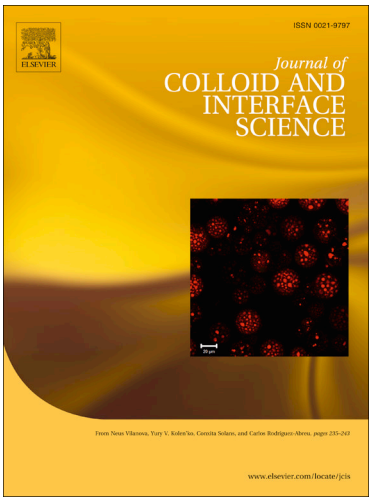

Enhanced selectivity and performance of heterogeneous cation exchange membranes through addition of sulfonated and protonated Montmorillonite

Farzaneh Radmanesh, Timon Rijnaarts, Ahmad Moheb, Morteza Sadeghi, Wiebe M. de Vos

PII: S0021-9797(18)31024-5
DOI: https://doi.org/10.1016/j.jcis.2018.08.100
Reference: YJCIS 24033

To appear in: *Journal of Colloid and Interface Science*

Received Date: 26 June 2018
Revised Date: 24 August 2018
Accepted Date: 27 August 2018

Please cite this article as: F. Radmanesh, T. Rijnaarts, A. Moheb, M. Sadeghi, W.M. de Vos, Enhanced selectivity and performance of heterogeneous cation exchange membranes through addition of sulfonated and protonated Montmorillonite, *Journal of Colloid and Interface Science* (2018), doi: https://doi.org/10.1016/j.jcis.2018.08.100

Enhanced selectivity and performance of heterogeneous cation exchange membranes through addition of sulfonated and protonated Montmorillonite

Farzaneh Radmanesh[a,b], Timon Rijnaarts[b], Ahmad Moheb[a], Morteza Sadeghi[a], Wiebe M. de Vos[b,*]

[a] Department of Chemical Engineering, Isfahan University of Technology, Isfahan 84156-83111, Isfahan, Iran

[b] Membrane Science & Technology, MESA+ Institute for Nanotechnology, University of Twente, P.O. Box 217, 7500 AE Enschede, The Netherlands

*Corresponding author: w.m.devos@utwente.nl

Abstract

Novel heterogeneous cation exchange membranes, based on poly (ether sulfone) and cation exchange resin, were prepared with the addition of protonated and sulfonated Montmorillonite (MMT) nanoparticles. Detailed investigations were then carried out studying the morphology, physical properties and the performance of membranes. It is observed that addition of MMT, leads to a substantially better distribution of ion exchange resin in the polymer matrix. This leads, at low loadings of MMT (0.5 wt%), to membranes that are more hydrated, more hydrophilic and with higher ion exchange capacities. Especially at these low MMT loadings, substantially better membrane performance is observed, with higher permselectivities, lower areal resistances and increased ion transport during electrodialysis. A very surprising effect is that the addition of MMT has a strong effect on the selectivity of the membranes, especially towards Mg^{2+}. A high affinity of the nanoclay towards Mg^{2+}, selectively slows down Mg^{2+} transport through the nanoclay containing membrane. At low MMT loadings this leads to a much higher areal resistance for Mg^{2+}, while for Na^{+} and Ca^{2+} the areal resistance is decreased. This leads to resistance based selectivities of 5.5 for Na^{+}/Mg^{2+} and 4.5 for Ca^{2+}/Mg^{2+}. Under more challenging electrodialysis operation selectivities become lower, but persist at 2.6 for Na^{+}/Mg^{2+} and 2.04 for Ca^{2+}/Mg^{2+}, outperforming commercial Ralex membranes. Overall, the protonated clay leads to slightly better membrane performances and selectivities than the sulfonated clay, likely due to a better compatibility with PES.

Keywords: Electrodialysis, Heterogeneous, cation exchange membrane, Montmorillonite, Ion selective

1. Introduction

Electrodialysis (ED) is a membrane-based separation technology applicable for the pre-concentration of brines [1, 2], the production of table salt [3], brackish water desalination [4], and organic acid production [5]. In ED, ion-exchange membranes (IEMs) that allow selective passage of counter-ions and inhibit passage of co-ions, are vital to the efficient operation [6].

Based on their structure, IEMs can be divided into two groups, homogeneous and heterogeneous, each with their own distinct properties. Heterogeneous membranes are made by dispersing ion exchange particles in an inert plastic binder while homogeneous membranes only consist of ion exchange type materials (polymer backbones with charged side-groups). In general, homogeneous membranes have good electrochemical properties but, are mechanically weak. Heterogeneous membranes, on the other hand have very good mechanical properties but show poorer electrochemical performance [7]. The desirable properties of an ion exchange membrane are high permselectivity, low electrical resistance, good mechanical, chemical, and thermal stabilities [8]. However, for specific applications (such as ED, Bipolar membrane ED or Reverse ED) priorities are given to certain properties. Variation of functional groups, selection of different polymeric matrices, polymer blending, adding various additives, alteration of cross-link density, and surface modifications are commonly-used methods to obtain ion exchange membranes [9] with the desired properties.

High selectivity among divalent and monovalent ions in IEMs is important for separations such as the softening of hard water and acid recycling from industrial wastewater containing metallic salts [10, 11]. However, ion-exchange membranes normally exhibit only low mono- to divalent selectivities [12]. Many researchers have investigated methods to improve the monovalent/divalent or monovalent/multivalent ion selectivity of ion-exchange membranes. These methods are based on the ionic size differences by tuning the degree of cross-linking, the affinity of the cations towards the membrane, and the difference in the migration speed (mobility) of the cations [1, 13-15]. For example, Sata and co-workers showed that the deposition of protonated polyethyleneimine (PEI) on cation-exchange membranes gave control over the hydrophobicity and cross-linking at the membrane surface and improved Na^+/Ca^{2+} selectivity up to 7 [1]. Abdu and coworkers modified Neosepta CMX cation-exchange membranes with PEI/poly (styrene sulfonate) (PSS) multilayers and changed the Na^+/Ca^{2+} selectivity from 0.64 to 1.5 [14].

In recent years, there has been considerable interest in using functional nanoparticles as additives to enhance the properties of IEMs. Nanoparticles not only influence the physio/chemical characteristics of the membrane and the separation properties such as permselectivity, ion-flux, conductivity, but also the mechanical and thermal stabilities of the polymeric membranes, thereby improving the membrane performance [16-18]. A nanoparticle with a wide range of applications is the nano-sized clay Montmorillonite. Montmorillonite (MMT) is an abundant and inexpensive layered silicate composed of tetrahedral silica and octahedral alumina sheets. MMT has unique properties including a high surface area, a two-dimensional structure, and a negative charge. Previous work has shown that MMT can be introduced into polymeric materials to create improved nano-composites materials [19]. To increase the capability to disperse MMT and to alter the transport properties of resulting membranes, an organic modification can be done. Several studies have been carried out using unmodified and sulfonated clay particles in direct methanol fuel cell membranes, such as Nafion, sPEEK, PVA, and PVDF membranes, leading to improvements in proton conductivity and reduced methanol permeability [19-23].

Some work, [24] and [25], has been dedicated to include nanoclay in heterogeneous cation-exchange membranes due to clay's suitable properties, such as easy availability, layered structure, hydrophilicity, low cost, and it’s cation exchange capacity. Namdari et al. [24] added montmorillonite K10 to PVC/HIPS/ABS blended heterogeneous cation exchange membranes. Hosseini et al. [25] focused on mixed matrix PVC based-co-clay nanoparticles heterogeneous cation exchange membranes and studied the effect of clay nanoparticles concentration on membrane electrochemical properties. Both studies showed that the addition of clay lead to a much better distribution of the IEX resin in the polymeric matrix. This leads to improved membrane properties of the prepared membranes, such as a higher ion exchange capacity (IEC), water content, permselectivity, and an lower electrical resistance. While Hosseini et al. [25] found an optimal clay concentration of 1%, Namdari et al observed an optimimum at 3%. These works where however limited to a single binder chemistry (PVC). Moreover no attempts were made to investigate the effects of these nanomaterials on the selectivity of the ionic transport of prepared modified IEMs.

Besides the properties mentioned above, nanoclays can have a different affinity for cations. In previous years, a lot of researches have been done with the aim of characterizing the ion-selective properties of nanoclay [36,27], as ion-exchange particles. Sposito et al. [27] showed that in the perchlorate medium, nanoclays shows a slight preference for Na^{+} over Ca^{2+}, Mg^{2+} over Na^{+}, and no preference for Mg^{2+} over Ca^{2+}.

However, they mentioned that the exchange isotherm of nanoclays depends strongly on the exchangeable sodium percentage (ESP), electrolyte concentration, and the mineralogy of clays [27]. We believe that the observed ion-selective nature of nanoclays, also makes them a promising choice for the preparation of cation selective ion-exchange membranes for water softening applications. Therefore, we present here the first study where the incorporation of clay on IEM's is studied and where the selectivity towards cations such as Na^{+}, Ca^{2+} and Mg^{2+} is taken into account. Moreover, this manuscript encompasses the first study to incorporate nanoclays into poly (ether sulfone) (PES) based heterogeneous cation membranes. For a complete picture, both protonated (OH-MMT) and sulfonated montmorillonite (HSO_3-MMT) particles were incorporated in a heterogeneous cation-exchange membranes based on poly (ether sulfone) (PES) as the polymeric matrix and Amberjet 1200D as the ion-exchange resin.

The effect of the HSO_3-MMT and OH-MMT concentration on the physico-chemical characteristics of prepared heterogeneous cation-exchange membranes were studied in detail. Here we have combined materials based characterizations such as degree of hydration, ion exchange capacity, contact angle and membrane morphology, with membrane performance measurements, such as permselectivity and resistances for sodium chloride, magnesium chloride, and calcium chloride. Our results indicate clearly, that membrane properties can be significantly improved by only a small addition of clay nanoparticles. Moreover, the addition of clay provides the membrane with a significant selectivity of sodium and calcium over magnesium.

2. Experimental

2.1 Materials

Poly (ether sulfone)(Mw=35000 g/mol) was obtained from BASF. Dimethylformamide (DMF) and Toluene (99.5%) were employed as solvents and were obtained from Merck chemical Co. MMT (Montmorillonite-K10, surface areas of 220-270 $m^2.g^{-1}$) was provided from Aldrich. The Cation exchange resin (Amberjet 1200D, strongly acidic cation exchanger in Na^+ form with a capacity of 1.8 meq/L) provided by by Merck Inc., Germany, was also used in membrane preparation. 3-Mercaptopropyl trimethoxysilane (3-MPTS) (95%) was purchased from Sigma. Other chemicals (NaCl, $MgCl_2$ hexahydrate 99% and $CaCl_2$ hexahydrate 0.99%) were supplied by Sigma-Aldrich. Throughout the experiments, deionized water (Milli Q, 18.2 MΩ.cm) was used to prepare the solutions.

2.2 Preparing protonated MMT and sulfonated MMT

The received Montmorillonite was treated with 0.5 M H_2SO_4 at 300 K to convert ONa-MMT into OH-MMT, and was then filtered and washed with deionized water. After drying at 90 °C under vacuum for 24 h, protonated montmorillonite (OH-MMT) was obtained. The surface functionalization of OH-MMT with 3-mercaptopropyltrimethoxy silane (3-MPTMS) was performed in toluene for 24 h with weight ratio of OH-MMT, 3-MPTMS, and toluene of 1:10:20. Then the thiol group (-SH) grafted onto MMT was oxidized into sulfonic acid (-HSO_3) using 10 wt. % hydrogen peroxide at 80 °C. The prepared MMT samples were then treated with 1 N H_2SO_4 at ambient temperature to complete the process. The treated MMTs were filtered, washed several times with deionized water and ethanol, and dried at 80 °C in a vacuum oven [19]. Fig. 1 describes the procedure used to prepare HSO_3-MMT.

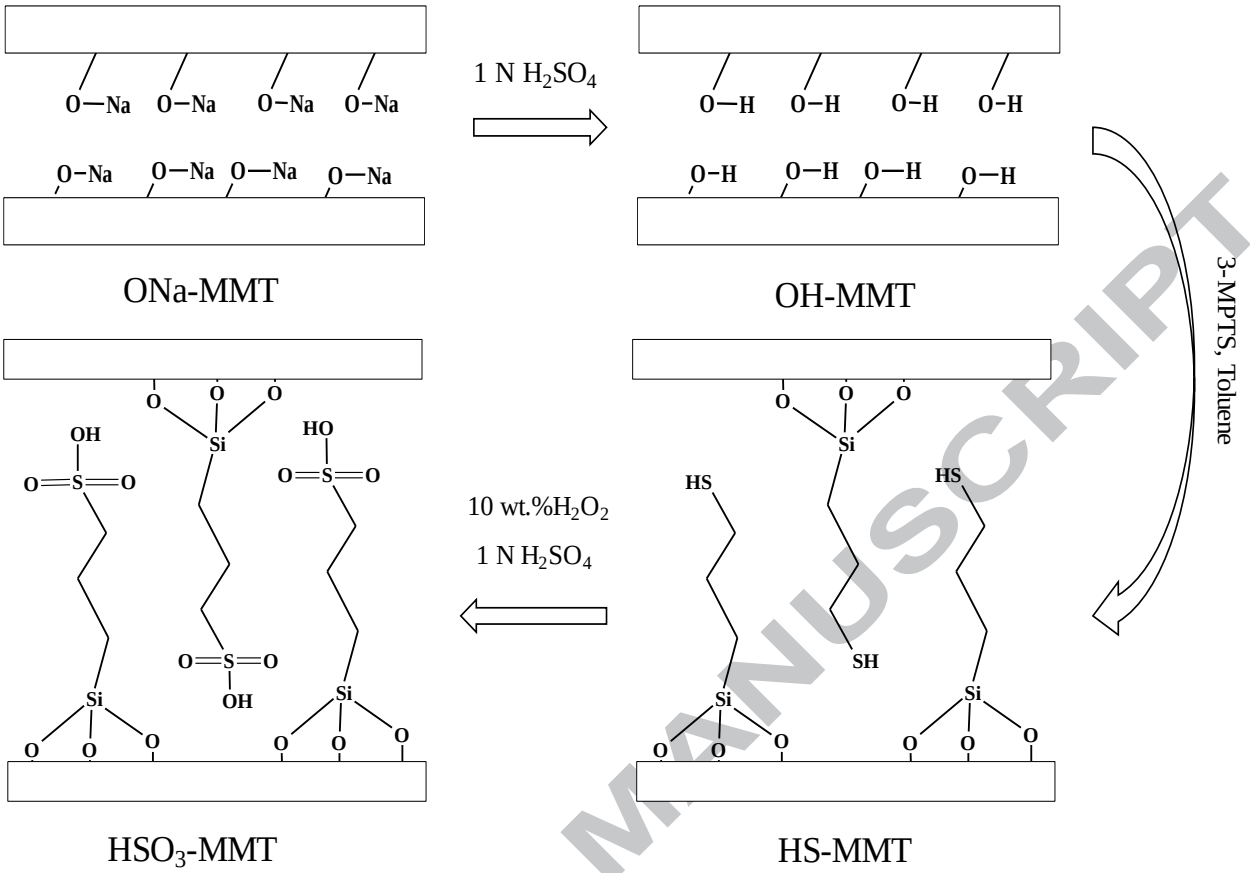

Figure 1. Schematic of the process for the preparation of sulfonated MMT.

2.3 MMT characterization

Fourier transform infrared (FTIR) spectra were obtained using a Jasco-680 (Japan) spectrometer at 4 cm^{-1} resolution at wave numbers of 400-4000 cm^{-1}. To determine the amount of introduced organic compounds in weight percent, thermogravimetric analysis (TGA) was performed on a STA503 win TA (Bahr Thermoanalyse GmbH, Hüllhorst, Germany) at the heating rate of 10 °C /min from 50 to 850 °C under nitrogen atmosphere.

2.4 Membrane preparation

The heterogeneous cation exchange membranes were prepared by dispersing cation exchange resin particles in polymeric solutions, followed by casting and solvent evaporation as described elsewhere [17, 28]. In short, the cation exchange resins were dried in an oven, powdered using a ball mill and then sieved (37-44 μm). This was followed by preparing the polymeric solutions by dissolving the PES polymer binder into DMF. Then powdered resin particles and varying amounts of OH-MMT or HSO_3-MMT (additives) were added to the solution. The mixtures were agitated at room temperature

overnight. For a better dispersion of particles and to break up aggregates, the mixture was sonicated. The mixture becomes more viscous and homogeneous during the sonicated process [29].The mixture was finally cast on a clean and dry glass plate and was allowed to completely dry at 55°C. As a final step, the prepared membranes were then immersed in a 0.5 M NaCl solution for 48 h. The membrane thickness was maintained around 60-80 µm. For all experiments, the ratio of resin to polymer and solvent to polymer were kept at 1/1 (w/w) and 20/1 (v/w). Weight percentages of OH-MMT and HSO_3-MMT in the membranes were 0, 0.5, 1, 2, 4, and 8 wt.%.

2.5 Membrane characterization

2.5.1 Scanning Electron Microscopic (SEM)

The membrane structure and the distribution of the resin particles were studied by scanning electron microscopy (JEM, using a JEOL JSM-6010LA). SEM was carried out by cutting samples into the desired size and mounting them on a holder using double-sided carbon tape. After chromium coating, SEM images were taken from the samples.

2.5.2 Contact angle

For quantitative measurement of the hydrophilicity or hydrophobicity of the membranes, contact angle was measured a contact angle measuring device (OCA 20, Data-physics, Germany).

2.5.3 Water content

The membrane's water content is obtained from the weight difference between the dry and wet membrane and is defined by equation (1):

$$\text{water content} = \frac{W_w - W_d}{W_d} \quad (1)$$

Here W_d and W_w are the dry and wet mass of the membrane, respectively. To measure W_w and W_d, the membrane was immersed in distilled water for 48 h at room temperature. Afterwards, the water remaining on the surface of the wetted membranes was wiped off with tissue paper and the membrane was weighed (W_w). The membrane was then dried at 60 °C until a constant weight was obtained as W_d [17].

2.5.4 Ion Exchange Capacity (IEC) and Fixed Ion Concentration (FIC)

The IEC can be measured using a conventional titration method [30]. The membrane was first immersed in a 0.006 M HCl solution for 48 h to exchange all cations with H^+ and was subsequently washed with de-ionized water to remove any excess of HCl. Afterwards, the membrane was immersed in a 0.1 M NaCl solution during 24 h to exchange the H^+ with Na^+. The resultant solution was then titrated with 0.006 M NaOH (C_{NaOH}) and a phenolphthalein indicator. The ion exchange capacity (IEC) was calculated by the following equation [17]:

$$IEC = \frac{C_{NaOH} \times V_{NaOH}}{W_d} \quad (2)$$

The Fixed Ion Concentration (FIC) can be obtained by Eq. (3).

$$FIC=\frac{IEC}{\text{water content}} \quad (3)$$

2.5.5 Membrane permselectivity

The membrane potential (the sum of Donnan and diffusion potentials) was evaluated using a two-compartment cell as described elsewhere [17, 18]. The cell was made from Pyrex glass and the sections were separated by the membrane. The concentrations of electrolyte (NaCl) on both sides (C_1/C_2) was kept constant (C_1 = 0.1 M and C_2 = 0.01 M). To minimize the effect of the boundary layer on the potential, both compartments were vigorously stirred by means of mechanical stirrers during the measurements. The developed potential difference across the membrane was measured using calomel electrodes and a digital multimeter (E_m).

The transport number of counter-ions (Na^+) through the membrane was calculated from the Nernst equation [31]:

$$E_{measured}=(2t_i^m-1)(\frac{RT}{nF})\ln(\frac{\alpha_1}{\alpha_2}) \quad (4)$$

Where t_i^m, T, R , F,n, and $(\frac{\alpha_1}{\alpha_2})$ are the transport number of the counter ions through the membrane, temperature, gas constant, Faraday constant, valence of counter-ion and activity coefficients ratio in the solutions in contact with both membrane surfaces determined by Debye-Huckel, respectively.
The potential was measured every 2 minutes until a constant value (E_m) was obtained. The experiment was repeated two times and the average value is reported. The ionic permselectivity (P_s) of membranes was calculated based on counter-ion migration through the ion exchange membrane [18, 32]:

$$P_s=\frac{t_i^m-t_0}{1-t_0} \quad (5)$$

Where t_0 is the cation transport number in the solution [33].

2.5.6 Electrical resistance

Membrane electrical resistance measurements were carried out in a setup reported elsewhere [34]. This setup was made of PMMA and consisted of six separate compartments which are separated by membranes. The membrane under investigation was placed in the middle position and was equilibrated with the measuring solution for at least 24 h. The other four membranes were commercial ion exchange membranes (cation exchange membranes CMX and anion exchange membranes AMX from Neosepta).

Measurements with a 0.5 M solutions of sodium chloride, Magnesium Chloride, and Calcium Chloride (compartments 3 and 4) were carried out with a potentiostat/galvanostat PGSTAT302N (Metrohm Autolab, The Netherlands), which applied a fixed current and simultaneously measured the voltage drop over the membrane under investigation. In both compartments adjacent to the central membrane (compartments 2 and 5), a 0.5 M NaCl solution to avoid influences of the electrode reactions at the working electrodes and in electrode compartments (1 and 6), a 0.5 M Na_2SO_4 was used. The anode and the cathode were made of titanium. All solutions were recirculated by the gear pumps (Cole-Parmer Instrument Co., Digital Gear Pump, USA) and experiments were performed at a temperature of 25°C. After applying the current via anode and cathode over the six compartment, the potential difference over investigated membrane was measured using the Haber–Luggin capillaries. These capillaries, filled with a 2 M KCl solution, were connected to a small reservoir which contains calomel reference electrodes (QiS, QM 712X, ProSense B.V., The Netherlands). The calomel reference electrodes were connected to a potentiostat. The final resistance was calculated by the slope of the current density versus voltage drop curve (R_1). In the next step, the membrane was removed and the electrical resistance was measured again (R_2). The membrane resistance (R_m) was obtained as the difference between R_1 and R_2.

2.5.7 Selectivity based on the resistance

To calculate the selectivity of the membranes (Na^+/Mg^{2+}) and (Ca^{2+}/Mg^{2+}), Eq. (6) was used:

$$\alpha_{a/b} = \frac{R_b}{R_a} \tag{6}$$

Where $\alpha_{a/b}$ is the membrane selectivity based on the resistance, $R_a$and R_b are the areal resistance ($\Omega.cm^2$) of the membrane to ion (a) and (b), respectively.

2.5.8 ED experiments

ED experiments were done using the test cell in section 2.5.6. The investigated membrane was clamped in the middle of a 6 compartment cell. Solutions with equal concentrations of 0.02 M NaCl, 0.01 M $MgCl_2$, and 0.01 M $CaCl_2$ (model river water) were placed on both sides of the membrane. The other four membranes were commercial ion exchange membranes (two CMX and two AMX). 0.05 M NaCl and 0.1 M Na_2SO_4 solutions were used as shielding solution and electrode rinsing solutions, respectively. Again, all solutions were recirculated. Samples were taken at specified times during ED to measure the conductivity and to calculate the selectivity from the re-circulation line.

The concentrations (mg/L) of cations were determined using ion chromatography (a Metrohm 850 Professional IC equipped with Metrosep C6-150/4.0 column). Each sample was measured two times and the average value was reported.

The limiting current was obtained based on I-V curve. As a result, the applied voltage was fixed at 8.0 V in order to operate below the limiting current density.

2.5.9 Measurements in ED experiments

Conductivity reduction (%) was obtained using equation (7):

$$\text{Conductivity reduction}=\left(\frac{k_i^0-k_i^t}{k_i^0}\right) \quad (7)$$

where k_i^0 and k_i^t are the dilute conductivities (mS/cm) at the beginning of experiment and at the time period t, respectively [17].

The ionic flux (J_i) through the cation exchange membrane can be calculated from the changes in concentration of the ions using equation (8) [14]:

$$J_i=\frac{V.\frac{dC_i}{dt}}{A} \quad (8)$$

where C_i is the concentration of the ions (mol/L) in the diluate compartment, A is the membrane surface area (m^2), and V is the volume of the compartments (L).

Another important parameter is the selectivity during ED performance. This parameter is a little different from what we discussed before in section 2.5.7. Selectivity based on the resistance gives us a sense about the selectivity of membrane but it is not a real process based selectivity from ED performance. To obtaining the selectivity for ED (S_j^i), the following equation was used:

$$S_j^i=\frac{\Delta C_i}{\Delta C_j}=\frac{\int J_i.dt}{\int J_j.dt} \quad (9)$$

Sodium concentration was twice times higher than calcium and magnesium concentration in ED experiments. To omit this effect in calculating ED based selectivity and be able comparing the results of sections 2.5.7 and 2.5.9, sodium flux was normalized in obtaining sodium selectivity to other ions.

2.5.10 Ion exchange isotherm

The ion exchange isotherm of membranes was measured in solutions of 0.5 M total salt concentration of pure salts and mixtures of NaCl, $MgCl_2$ or $CaCl_2$ following the procedures described earlier [35, 36]. Fist, the membranes were immersed in solutions for 48 hr. Afterward, the excess solution was wiped off with filter paper quickly, in a way that the electrolyte in the membrane was not removed. The membranes were then cut into the desired size and were mounted on SEM holders using double-sided carbon tape. All samples were dried in a vacuum oven overnight and sputter-coated with 10 nm of chromium prior to EDX analysis. EDX analysis was performed at 10 kV with >1000 counts/sec. The experiment was repeated four times and the average value was reported.

3. Results and discussion

The results and discussion section is split into three distinct parts. Initially, we study the characteristic properties of the clay particles used in our investigation. In the second part, we characterize membrane properties such as morphology (SEM), water content, contact angle and the ion-exchange capacity. In the third section the IEM's are characterized for their performance, studying permselectivity, resistance and selectivities.

3.1 Characterization of nanoclay

Table 1 shows a short review of all quantitative methods used for the characterization of OH-MMT and HSO_3-MMT. Each method shows good agreement with the others. Furthermore, FTIR spectra were taken to characterize the clay before and after surface modification. These spectra show a clear indication that sulfonation was successful, as can be found in the supporting information (SI.1).

The elemental analysis (EA) provided the sulfonation degree on the MMT surface. Based on the sulfur contents, the amount of sulfonated 3-MPTS detected is 0.56 mmol/g which has a good agreement with the ion-exchange capacity (IEC) obtained from titration of HSO_3-MMT (0.55 mmol/g). This IEC also matches those observed in earlier studies which obtained 0.52 mmol/g [19].

The thermal stability of OH-MMT and HSO_3-MMT was studied by thermogravimetric analysis (TGA), of which details are provide in the SI, section SI.1. With OH-MMT as the baseline, the amounts of functionalized groups in MMT could be evaluated to be 10 wt%. This value represents the loadings of organic functions and shows good consistency with the sulfur contents of 1.9 wt.% obtained by elemental analysis, which comes to a total degree of functionalization of 9.5%.

Table 1. An overview of the outcomes of several methods used for characterization of OH-MMT and HSO_3-MMT

Sample	EA analysis (%)			IEC based on EA (mmol/g)	IEC based on titration (mmol/g)	Degree of functionalization (%) based on EA	Degree of functionalization (%) based on TGA
	C (wt.%)	S (wt.%)	H (wt.%)				
OH-MMT	0.05	0.05	0.91	-	0.26	0	0
HSO_3-MMT	1.6	1.9	1	0.56	0.55	9.5	10

3.2 Membrane properties

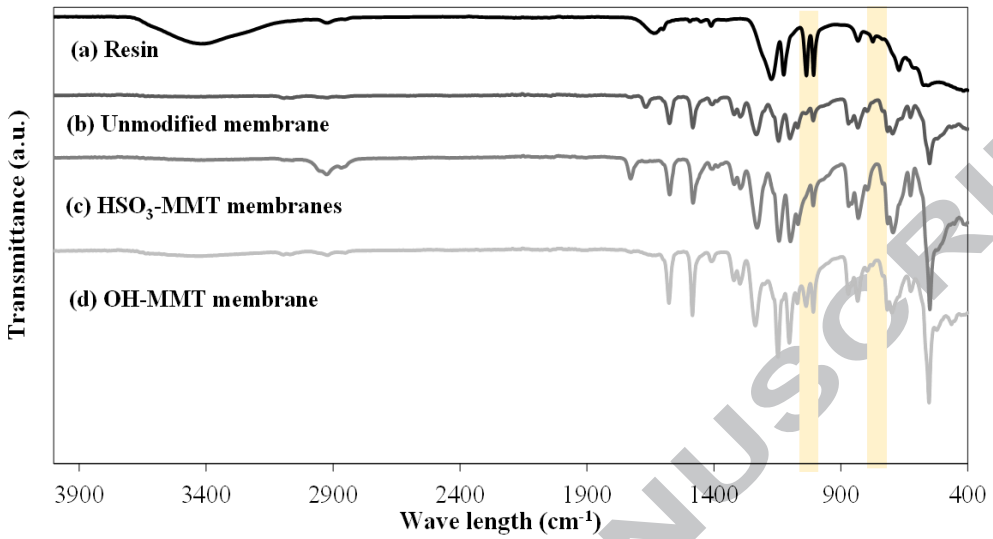

3.2.1 ATR-FTIR of membranes

Figure 2. FTIR spectra of (a) resin particles, (b) Unmodified membrane, (c) HSO_3-MMT membrane, and (d) OH-MMT membrane

Heterogeneous IEMs were prepared on the basis of PES, cation exchange resin particles and various amounts of modified and unmodified clay nanoparticles. FT-IR spectra of resin particles and of unmodified and modified membranes are shown in Figure 2. For unmodified membranes (2b), the peak at 1037 cm^{-1} can be attributed to the stretching vibrations of the SO_3 sulfonic [37]. By comparing the FTIR spectrum of protonated and sulfonated MMT IEMs (2c and 2d), it was found that the OH-MMT membrane spectrum has two more peaks at 1037 cm^{-1} and 770 cm^{-1} which can be related to the resins particles (Figure 2a). This indicates that OH-MMT membrane had more resin on its surface, while for the HSO_3-MMT membranes, PES and HSO_3-MMT dominate the surface of the membrane.

3.2.2 Morphological studies

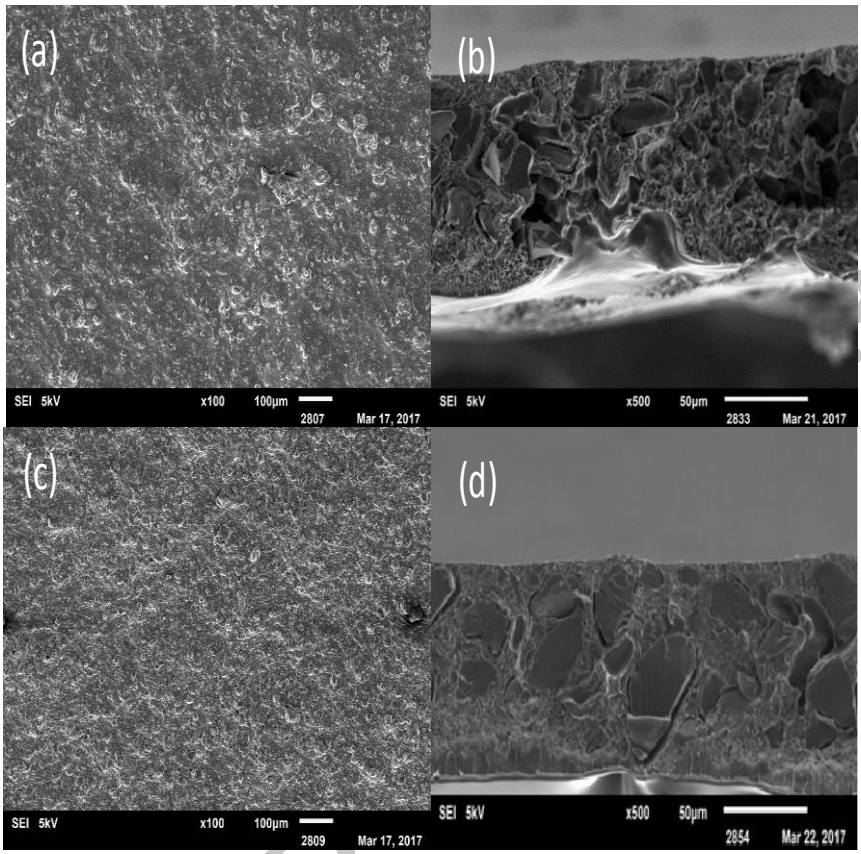

Figure 3. SEM images of surface (x100) and cross section (x500) of unmodified membrane (top) and 0.5 wt.% OH-MMT membrane (bottom).

A scanning electron microscopy study was carried out to investigate the distribution of resin particles in the membranes (Figure 3a and c). The polymer binder (non-conducting region) and ion exchange resin particle (conducting region) are clearly seen in the images. The resins are observed as dark gray areas in the SEM image of the membrane's cross section (x500). As can be seen, adding nanoclay led to a more uniform distribution of resin particles on the membrane surface. A uniform distribution of ion exchange particles on the surface and in the bulk of membrane matrix is important to the functioning of the membrane. It provides more conducting surface area and easy channels for counter-ion transportation [17]. Moreover, the unmodified membrane has cavities and pores unlike modified membranes, which has a dense structure (Figure 3.b and d). PES is a relatively hydrophobic polymer and the ion exchange resin is relatively hydrophilic. Silicate clays are hydrophilic and by protonating or sulfonating them, they become even more hydrophilic[38]. By adding MMT to the casting solution, a hydrophilic matrix was produced and a better compatibility between polymer binder and resin particles was

achieved. As a result, cavities and pores disappeared in modified membranes and a denser structure shows up. Similar observations were found for PVC based ion exchange membranes with added clay nanoparticles [24, 25]. Our results this demonstrate that this is a more generic effect, and it is likely that this effected can be replicated with many combinations of clay and polymer.

To study the membrane morphology in more detail, SEM of cross-sections were carried out at a 6000 magnification (Figure 4). The nanoclay (shown with white arrows) appears to be more finely dispersed at lower loading ratios and as the loading increases larger agglomerates emerge. SEM images of 0.5 wt.% and 2 wt.% OH-MMT and HSO_3-MMT membranes (Figure 4) confirm a good distribution of MMT in the polymer matrix. Unlike the membranes with low loading ratios, the SEM images of 8 wt.% OH-MMT and HSO_3-MMT clearly display nanoclay aggregation (shown with white circles). Good dispersion of resin and nanoclay particles would result in a more uniform distribution of ionic sites which improves the electrochemical properties of the membranes [17]. In addition, a good compatibility between nanoparticles and polymer chains can be seen. Also, FE-SEM micrographs (40000 magnification) are presented in SI. 2 which shows more agglomeration for HSO_3-MMT compare to OH-MMT nanoparticles in the polymeric matrix. These observations will be important to interpret the results in the next sections.

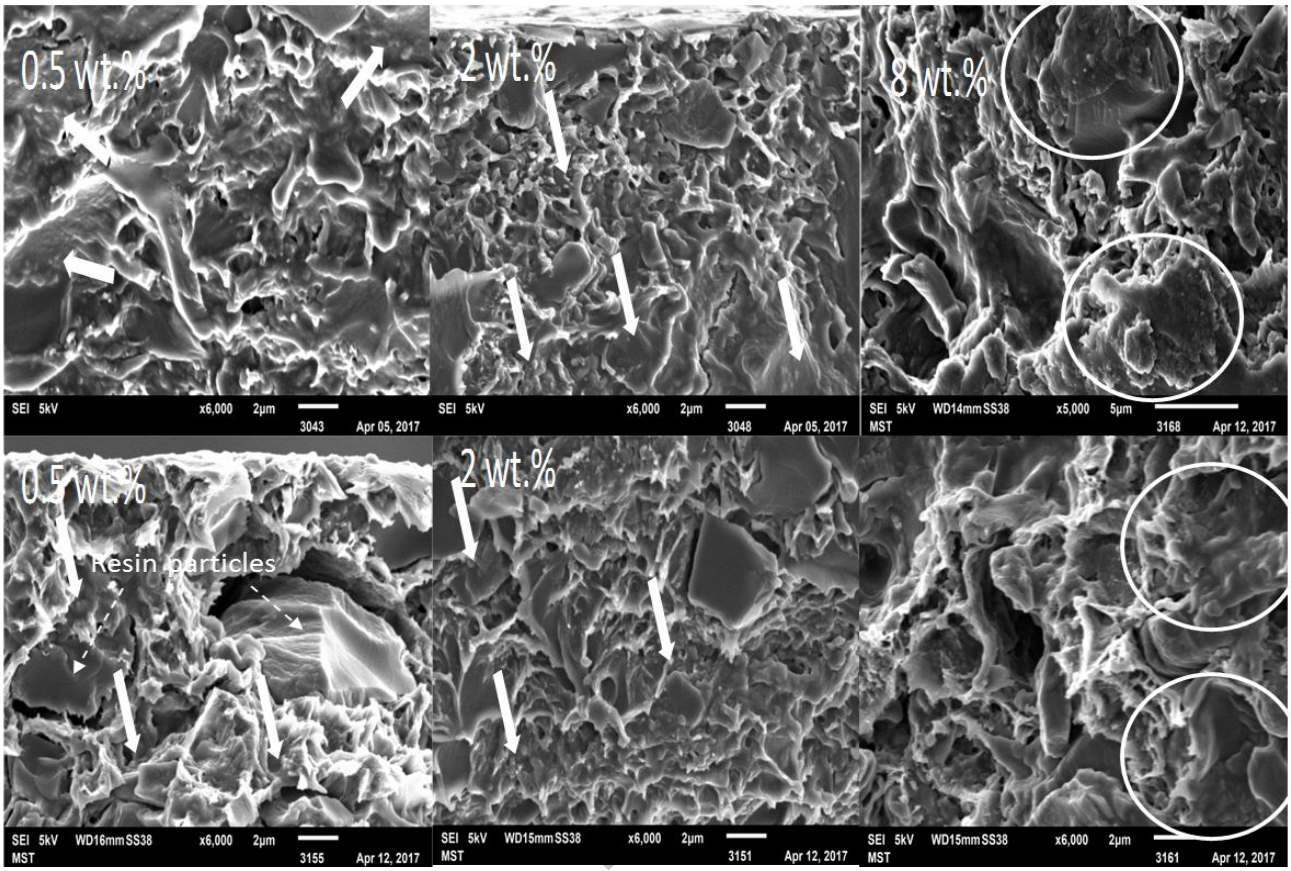

Figure 4. SEM images of membrane cross section at 6000 magnification (top: OH-MMT and bottom: HSO_3-MMT membranes)

3.2.3 Water content and contact angle

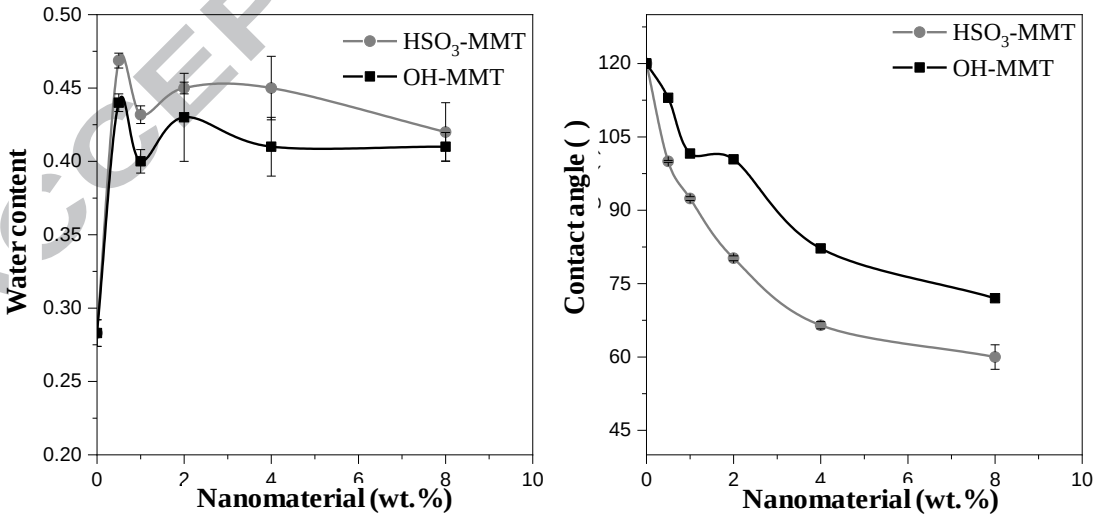

(a) (b)

Figure 5. Effect of nanoclay content on the water content of prepared membranes (a) and contact angle (b) of prepared membranes. All the experiments were repeated three times, error bars represent the standard deviation from the average.

The mechanical stability and cation selectivity of an ion-exchange membrane depend on the water content. In figure 5, we observe the water content (5a) and contact angle (5b) as a function of the percentage of added clay. As shown in figure 5a, a dramatic increase of water content results from adding nanoclay and functionalized nanoclay up to 0.5 wt.% in the casting solution. It is encouraging to compare this figure with that found by Namdari et al. [24] and Hosseini et al. [25] who found that membrane's hydrophilicity was enhanced up to 1 wt.% nanoclay but then decreased significantly. In our PES based IEMs the increase in water content remains over a much wider range of clay concetrations. The hydrophilic nature of nanoclay and their high affinity toward water play an important role, which leads to an increased in water content and water diffusion [17, 39]. Moreover, the better dispersion of the ion-exchange resin (figure 3) could allow the material to be better structured for water uptake. A high water content can provide more transfer channels for co- and counter ion transportation and as a result decrease the selectivity [18]. But this is not always true and depends on the membrane structure and its properties. With a further increment of nanoclay concentration from 0.5 to 8 wt.% no significant changes in water content was observed.

The membranes containing sulfonated nanoclay have a slightly higher water content compared to protonated membranes. This may be attributed to HSO_3 group of sulfonated MMT that makes the membrane more hydrophilic, and the higher ion exchange capacity of HSO_3-MMT (see table 1).

Apparently, adding as little as 0.5 wt.% of nanoclay to the casting solution, leads to a very large water content increase, while further addition did not have any considerable effect on the water content of membranes. This could indicate that the improved dispersion of ion-exchange resin, already observed at low nanoclay content, could be the major mechanism for additional water uptake.

The contact angle is a measure for the wettability and thus the hydrophilicity of the membrane surface. If the contact angle is below 90°, the surface is considered to be hydrophilic and if the contact angle is above 90°, the surface is considered to be hydrophobic [40]. The contact angle of the membrane as a function of the nanoclay concentration is shown in Figure 5b. The addition of clay leads to a decrease in membrane contact angle from 120°, for membranes without nanoclay, to 72 and 60 degrees, for membranes with 8% nanoclay. The decreasing trend of contact angle is due to the hydrophilic nature of the nanoclay. The difference between the contact angle of

membranes prepared with protonated and sulfonated nanoclay can be attributed to the fact that the functionalized nanoclay with HSO_3 is more hydrophilic.

3.2.4 Ion exchange capacity (IEC)

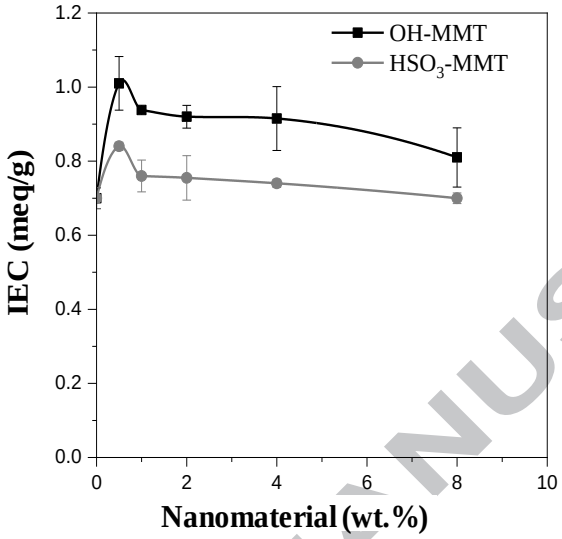

Figure 6. Effect of nanoclay content on the ion exchange capacity of prepared membranes, for OH-MMT and HSO_3-MMT. All the experiments were repeated three times, error bars represent the standard deviation from the average.

The IEC as a function of nanoclay content is shown in Figure 6. The IEC is initially enhanced by the addition of nanoclay and sulfonated nanoclay while a further addition lowered it. The highest IEC was obtained with the nanoclay concentration of 0.5 wt%. These results agree with the findings of other studies which IEC enhanced with the addition of sulfonated and unmodified nanoclays to ion exchange membranes [21,25]. They attributed this enhancement to the adsorption characteristic of nanoclays which facilitates the ion transports between membranes and solutions. Also, modification of nanoclays played an important role in improvement of IEC [21,25]. Moreover, a better dispersion of the ion-exchange resin leads to a better accessibility of charge groups. The ion exchange capacity was decreased again in additive concentration of 0.5 to 8 wt.%. At high nanoclay loadings, the accessibility of functional groups (resin) can decline as resin particles become surrounded by nanoclays, or because of nano-clay aggregation. This result is in line with the investigation of Hosseini et al. [25] which found that IEC decreased again with the addition of nanoclay between 1 wt.% to 8 wt.%.

The main purpose of functionalizing MMT with HSO_3 groups, in this research, was to provide a higher IEC. Indeed, the HSO_3-MMT has double the IEC of the OH-MMT(the

IEC of OH-MMT and HSO_3-MMT are 0.26 and 0.55 meq/g, see Table 1. Unexpectantly, as can be seen in figure 6, membranes containing OH-MMT have a higher IEC compared to the HSO_3-MMT. As described earlier, OH-MMT has a better compatibility with PES which would lead to better dispersion in the polymeric matrix. On the other hand, we expected that HSO_3-MMT preferred to gather near hydrophilic spots, resins particles, in the matrix. This phenomenon would result in membrane channel filling, lowering the access of counter ions to the functional groups [41], and thus lowering the IEC. Also, as discussed in section 3.2.1, OH-MMT membranes have more resin particles on their surface and exchanging of ions in these membranes are much easier compared to HSO_3-MMT ones.

The addition of clay can enhance the IEC, however, due to swelling (Higher water content of HSO_3-MMT than OH-MMT) the effective charge concentration in the matrix does not change for H^+, and even decreases for SO_3^- (can be seen in the section SI.4).

3.2.5 Ion exchange isotherms

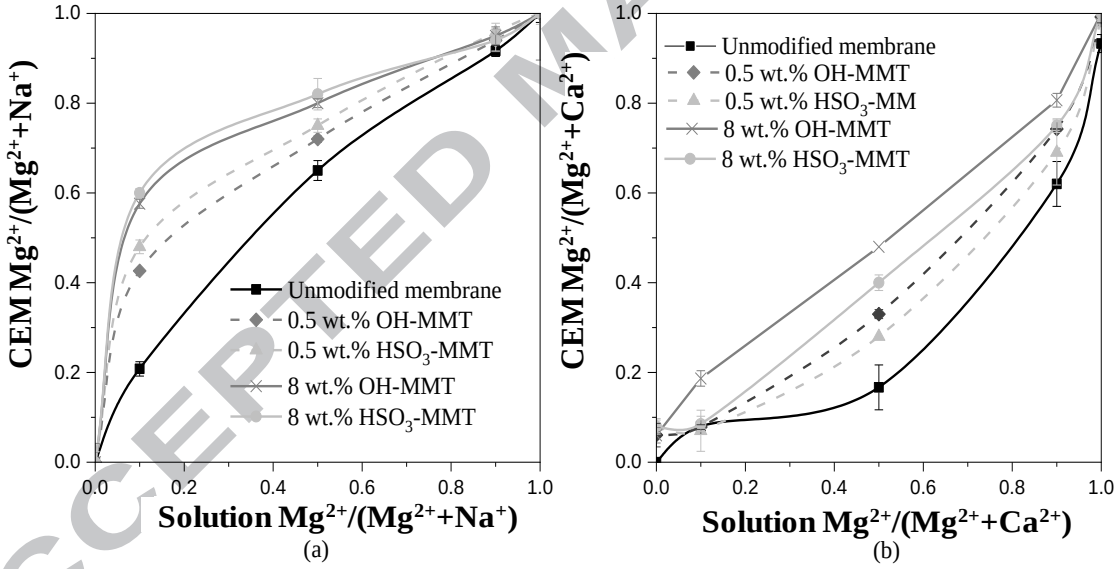

Figure 7. Ion exchange isotherms (a) in NaCl and $MgCl_2$ solutions and (b) in $CaCl_2$ and $MgCl_2$ solutions. All the experiments were repeated three times, error bars represent the standard deviation from the average.

Ion exchange membranes are used in different applications where multicomponent solutions are treated, such as demineralization of saline water, desalination of cheese whey solutions, production of sodium chloride from sea water, etc. [7]. The affinity of counterions for ion exchange membranes are variable and can affect the selectivity of

IEMs. Ion exchange isotherms are a criteria to determine the relative membrane affinity of salts and other solutes [35].

Ion exchange isotherms of prepared membranes in two binary solutions (NaCl, $MgCl_2$ and $CaCl_2$, $MgCl_2$) are presented in figure 7. Unmodified membranes show a small preference toward Mg^{2+} relative to Na^{+}. Interestingly, adding just 0.5 wt. % nanoclay increases the affinity towards Mg^{2+}, while more nanoclay (8 wt.%) enhances this effect.

In a $CaCl_2$ and $MgCl_2$ solution, the unmodified membrane has a strong affinity toward Ca^{2+}. With increasing nanoclay content, this affinity decreases until a small affinity for Mg^{2+} becomes apparent.

Clearly, nanoclay increases the affinity of membranes toward Mg^{2+} in binary solutions of (NaCl, $MgCl_2$) and ($CaCl_2$, $MgCl_2$). These changes in affinity of membranes are related to the nature of nanoclay. Potentially, this affinity could change the ion selectivity of the produced IEMs.

3.3. Membrane performance

3.3.1 Permselectivity

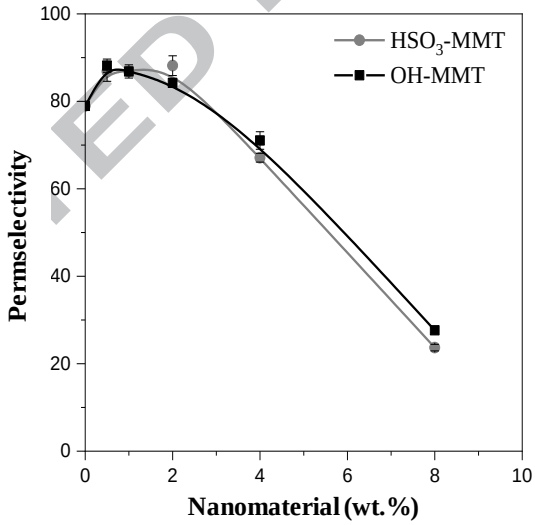

Figure 8. Effect of nanoclay content on the permselectivity of the prepared membranes for OH-MMT and HSO_3-MMT. All the experiments were repeated three times, error bars represent the standard deviation from the average.

Permselectivity is a property that shows the ability of a membrane to transport counter-ions, and to block co-ions. Figure 8 shows the permselectivity of the produced IEMs with added protonated and sulfonated MMT. By adding nanoclay up to 0.5 wt.%, the

permselectivity is significantly enhanced. As described in section 3.2.2, the modified membranes were found to have a denser structure in comparison to unmodified one and a more uniform distribution of resin in the polymer matrix. This improves the permselectivity. Possibly, nanoclays also fill and narrow the channels within the membrane which could increase the influence of functional groups on ionic transport [42]. However, increasing the clay content up to 4 and 8 wt.%, reduces the permselectivity very significantly. In part this can be explained by agglomeration of the nanoclay particles, which reduces the availability of functional groups [28, 43]. But the reduction in permeselectivity is so strong, that agglomeration likely also causes defects in the membrane which can be seen in SI. 2 and Figure 4. As can be seen in the Figure 8, sulfonation of nanoclay has a negligible influence on the permselectivity of membranes compared to the protonated nanoclay.

A clear optimum in performance is thus observed with the addition of just 0.5% of nanoclay. This optimum is found at significantly lower concentrations than was observed for the blending of nanoclay with IEMs using PVC as a binder [24, 25]. It seems that much less nanoclay is required when using PES as a binder to achieve a good distribution of ion exchange resin, that leads to better IEM performance.

3.3.2 Membrane electrical Resistance

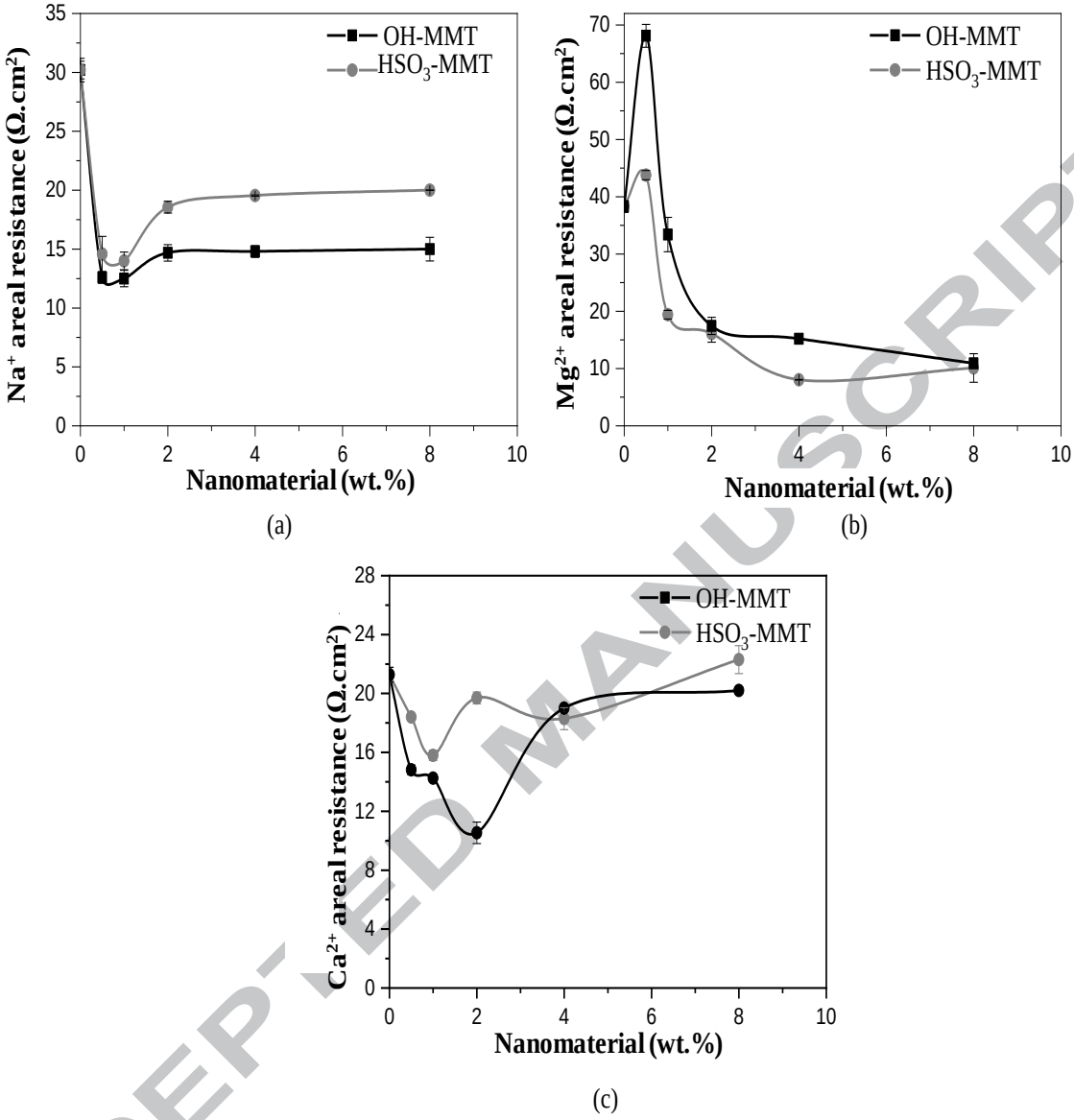

Figure 9. The areal electrical resistance of prepared cation exchange membrane for Na^+ (a), Mg^{2+} (b), and Ca^{2+} (c). All the experiments were repeated three times, error bars represent the standard deviation from the average.

The energy consumption of an ED process is dependent on the resistance of the solutions and IEMs. Thus, membranes with low electrical resistance are preferable for ED operation. Moreover, resistance is a tool which makes it possible to obtain insight into the selectivity of membranes for different cations. The resistance of IEMs depends on several parameters such as the membrane thickness and water content [44]. In figure 9, we show areal resistances towards Na^+, Mg^{2+}, and Ca^{2+}. From Figure 9a, it can be concluded that the membrane areal resistance for Na^+ decreases with increasing nanoclay content quite

strongly up to 0.5 wt.%. These results are in line with the water content and IEC results. As explained in section 3.2.3 and 3.2.4, water content and IEC, both increase significantly with a nanoclay content of just 0.5 wt.%. The water content and the IEC have an important impact on membrane resistance. Ion transportation through the membrane matrix improves when the water content and the IEC increases. This results in a reduced resistance [45]. The obtained sodium resistance for 0.5 wt.% OH-MMT membrane is around 12.5 $\Omega.cm^2$ which is comparable to the resistance of Ralex CMH-PES (MEGA, Czech Republic) membranes (9.8 $\Omega.cm^2$) [46]. The sodium areal electrical resistance increases, however, for a larger nanoclay content when going from 0.5 to 8 wt.%. These results are in a good agreement with the results of the IEC in section 3.2.4 where at these contents the IEC decreases. This causes the ions transportation to become more difficult and increases the sodium areal resistance. It is good to mention that HSO_3-MMT membranes have a lower IEC than OH-MMT membranes which leads to a slightly higher Na^+ resistance.

Figure 9b shows the Mg^{2+} areal resistance of membranes. Adding nanoclay up to 0.5 wt.% increases Mg^{2+} resistance quite strongly. This may be due to the increment of the IEC in the same loading ratio as explained in section 3.2.4. By enhancing the IEC of the membrane, the movement of multivalent ions can be hindered [10]. This is especially true when the ion binds strongly to the ion-exchange groups, slowing down transport. Mg^{2+} resistance, however, decreases at higher additive concentrations. Again, this trend is consistent with the results of IEC in section 3.2.4. Moreover, HSO_3-MMT membranes havea lower Mg^{2+} resistance compared to OH-MMT membranes. This may be due to the difference in the affinity of Mg^{2+} for the two types of nanoclay.

Figure 9c presents Ca^{2+} areal resistance of membranes. The change of Ca^{2+} areal electrical resistance as a function of nanoclay content is similar to Na^+. This could be related to the similarities between the two ions like the similar hydrated radius [47]. Still it is very unexpected that the two di-valent cations, Mg^{2+} and Ca^{2+}, behave so differently. In figure 7b, we did show that the addition of nanoclay, leads to a relative increase in Mg^{2+} affinity. This indicates that it is specifically the high affinity of the nanoclay towards Mg^{2+} in binary solution of $MgCl_2$ and $CaCl_2$ that leads to the high resistance of the membrane for Mg^{2+} transport, rather than just the observed increase in IEC. For Ca^{2+} the affinity towards the nanoclay is much smaller, and as such a more similar behavior to Na^+ is observed.

3.3.3 Selectivity based on resistances

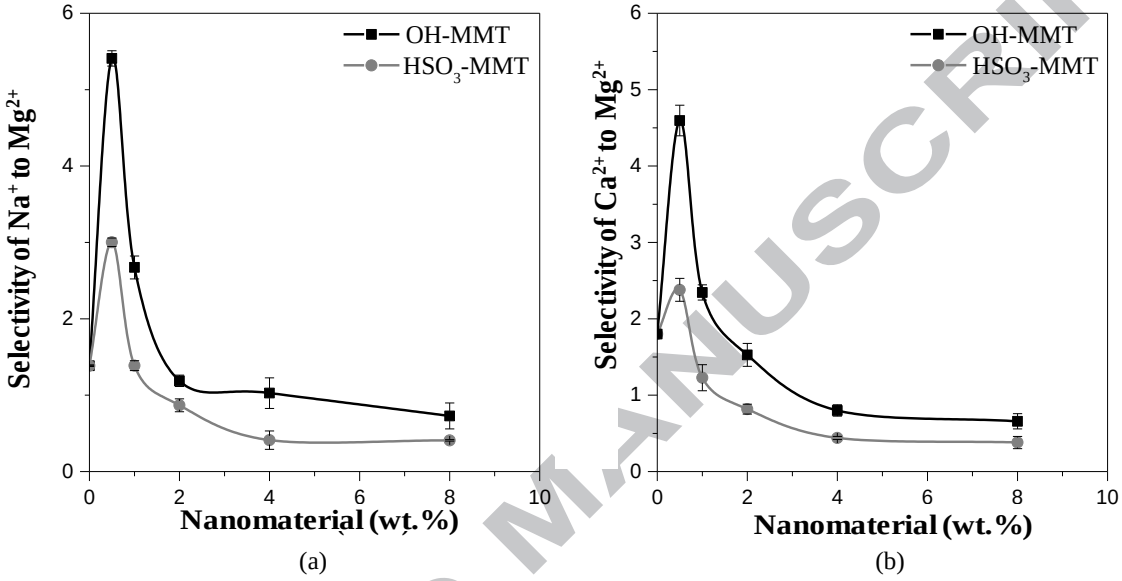

Figure 10. Selectivities of Sodium to Magnesium (a) and Calcium to Magnesium (b), based on their respective areal resistances. All the experiments were repeated three times, error bars represent the standard deviation from the average.

Selectivities were calculated based on the resistances (Equation 6). Figure 10a shows the Na^+ to Mg^{2+} selectivity of prepared membranes. Both types of membranes show the same trend for monovalent selectivity with increasing nanoclay loading. The selectivity for sodium initially increases substantially by the addition of nanoclay, up to a selectivity of about 5.5, while a further addition of nanoclay (1 wt.%) lowers it again. We attribute this phenomenon to entrapment of Mg^{2+} in the membrane due to its high affinity for the nanoclay as explained in the previous section. However, with increasing nanoclay content from 0.5 wt.% to 8 wt.%, membrane defects and nanoclay agglomeration cause the selectivity to decrease, just as the permselectivity decreased at higher nanoclay content.

Selectivity of Ca^{2+} to Mg^{2+} is presented in figure 10b. Utilizing MMT in the casting solution up to 0.5 wt. % leads to an increase in selectivity of Ca^{2+} to Mg^{2+}, very similar to the effect observed for Na^+ and Mg^{2+}. As discussed, and as observed in figure 7, the affinity for the nanoclay is much higher for Mg^{2+} than for Ca^{2+}. Just as for Na^+/Mg^{2+} the

selectivity of Ca^{2+} to Mg^{2+} decreased by a further increase in additive concentration from 0.5 to 8 wt.% in the prepared membranes. Again, this is likely due to nanoclay agglomeration, and membrane defects that result from that.

In conclusion, our IEM prepared with 0.5 wt.% OH-MMT has the highest selectivity of Na^{+} to Mg^{2+} which is higher than that of commercial Ralex CMH-PES (MEGA, Czech Republic) membranes which have a selectivity of 2.3[48]. Surprisingly, modified membranes with nanoclay also show a selective behavior for Ca^{2+} over Mg^{2+} and again 0.5 wt.% OH-MMT membrane shows the highest selectivity. This is the first time that such selectivities have been demonstrated for nanoclay enhanced IEM's, and opens a new a promising route towards more selective membranes.

3.3.4 Membrane performance in ED

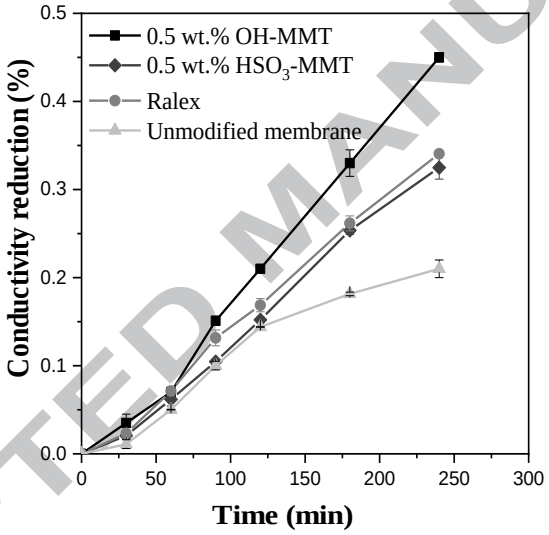

Figure 11. Conductivity reduction versus time, during ED operation. All the experiments were repeated three times, error bars represent the standard deviation from the average.

For ED experiments, a mixture of salts with the concentration of 0.02 M NaCl, 0.01 M $MgCl_2$, and 0.01 M $CaCl_2$ was used for the initial concentration. During a 4 hour experiment, samples were taken in specified times to calculate conductivity reduction and ED based selectivity from Equations 7 and 9.

The conductivity reduction is a criteria showing the desalination rate of the membranes. The conductivity reduction for the unmodified membrane and the best membranes from each kind of modification (0.5 wt.%) are shown in Fig. 11. Also, for comparison a CMH-PES Ralex membrane with the dry thickness of 0.65±0.05 mm was tested under the same conditions. The conductivity reduction increases with time for all type of membrane and

the highest conductivity reduction was obtained for 0.5 wt. % OH-MMT membrane. This is due to its high IEC and permselectivity. Remarkably, the desalination rate of this membrane is higher than the commercial Ralex membrane. The lowest conductivity reduction is for unmodified membrane because of its lower permselectivity and high resistance compared to other membranes.

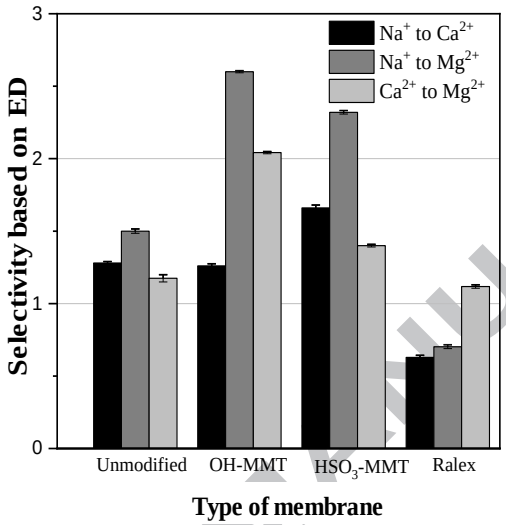

Figure 12. Membrane selectivity based on ion transport during ED operation. All the experiments were repeated three times, error bars represent the standard deviation from the average.

During ED, cations pass through the membrane and reach to the concentrated section. However, the ion flux depends on the type of ion, leading to a certain selectivity. Figure 12 shows the selectivities of unmodified membrane and the best membranes from each kind of modification (0.5 wt.%). Again, selectivities of Ralex were measured in the same condition. The highest selectivities for sodium to magnesium and as well for calcium to magnesium were obtained for the 0.5 wt.% OH-MMT membrane. 0.5 wt.% HSO_3-MMT and even unmodified membranes represented higher selectivity of sodium to magnesium and calcium to magnesium than the commercial membrane. These selectivities are in lower than those in section of 3.3.3., but do show that these Na^+/Mg^{2+} and Ca^{2+}/Mg^{2+} selectivities persist under conditions relevant to true applications.

4. Conclusion

The aim of this work was to study and to enhance the transport properties of poly (ether sulfone) based heterogeneous cation exchange membrane by the addition of nanoclay.

Moreover, we study for the first time the ionic selectivity that results from the embedding of nanoclay in the membrane, and compare the effect of two nanoclays with different surface chemistries. For both OH and HSO_3 functionalized Montmorillonite, already a small addition of the clay (0.5 wt.%) is found to be enough to lead to an improved resin distribution in the membrane, as observed by SEM. A further addition of nanoclay, however, leads to the formation of undesired nanoclay clusters. These observations on our PES based membranes are in line with previous observations of the addition of clay to PVC based heterogeneous IEMs [24,25].

The permselectivity, water content, transport number, and IEC were enhanced through the addition of nanoclay (OH-MMT and HSO_3-MMT) upto 0.5 wt.%, as expected from the better resin distribution. For higher nanoclay contents, these properties decrease. The formation of nanoclay clusters can lead to membrane defects that lower the membrane performance. A similar effect is observed for the Na^+ and the Ca^{2+} resistance of the membranes, that initially decrease substantially with just a small fraction of nanoclay (0.5 wt.%) and then increase again by further addition of nanoclay from 0.5 to 8 wt.%. However, for Mg^{2+} a very different behavior was observed. For Mg^{2+} the resistance strongly increased at 0.5% nanoclay, and then decreased again upon further loading. This effect can be attributed to the increased affinity of the membrane towards Mg^{2+} due to the addition of clay, as determined by separate ion-exchange isotherms. The high affinity for Mg^{2+} leads to the higher resistance, as a strong affinity of the membrane for a specific ion will slow its transport through the membrane. The large difference in resistance between Na^+ and Ca^{2+} on one hand, and Mg^{2+} on the other, leads to very interesting ion selectivities, and shows for the first time the large potential of clay as a membrane additive to achieve ionic selectivities. These selectivities did decrease somewhat under ED measurements at a stack level, but they do persist under conditions relevant to true applications.

For all electrochemical and performance properties, HSO_3-MMT membranes exhibited the same trend as OH-MMT membranes, but the OH-MMT membranes performed better both in selectivities and in areal resistance. Overall, the membrane with 0.5 wt.% OH-MMT showed the best results for water content, permselectivity, and IEC. Moreover, this membrane showed a much improved (lower) membrane resistance towards Na^+ permeation. Finally, it achieved the highest Na^+ and Ca^{2+} cations selectivities toward Mg^{2+} with values of 5.5 and 4.5 based on resistances and selectivities of 2.6 and 2.04 based on ED stack measurements. Both in selectivity and ion transport, our 0.5 wt.% OH-MMT membrane outperformed a commercial Ralex membrane.

Our work shows for the first time that additives such a nanoclay, will not only lead to improved transport properties in heterogeneous IEMs, but can also lead to remarkable selectivities toward specific ions. This opens the door to new studies with different nanoclays and additives to develop IEMs with improved selectivities catering to specific apllications such as waste water management and water softening.

References

[1] T. Sata, T. Sata, W.K. Yang, Studies on cation-exchange membranes having permselectivity between cations in electrodialysis, J Membrane Sci, 206 (2002) 31-60, https://doi.org/10.1016/S0376-7388(01)00491-4.
[2] M. Reig, S. Casas, C. Aladjem, C. Valderrama, O. Gibert, F. Valero, C.M. Centeno, E. Larrotcha, J.L. Cortina, Concentration of NaCl from seawater reverse osmosis brines for the chlor-alkali industry by electrodialysis, Desalination, 342 (2014) 107-117, https://doi.org/10.1016/j.desal.2013.12.021.
[3] Y. Tanaka, R. Ehara, S. Itoi, T. Goto, Ion-exchange membrane electrodialytic salt production using brine discharged from a reverse osmosis seawater desalination plant, J Membrane Sci, 222 (2003) 71-86, https://doi.org/10.1016/S0376-7388(03)00217-5.
[4] G.M. Geise, H.S. Lee, D.J. Miller, B.D. Freeman, J.E. Mcgrath, D.R. Paul, Water Purification by Membranes: The Role of Polymer Science, J Polym Sci Pol Phys, 48 (2010) 1685-1718, |https://doi.org/10.1002/polb.22037.
[5] C. Huang, T. Xu, Y. Zhang, Y. Xue, G. Chen, Application of electrodialysis to the production of organic acids: state-of-the-art and recent developments, J Membrane Sci, 288 (2007) 1-12, https://doi.org/10.1016/j.memsci.2006.11.026.
[6] R.W. Baker, Membrane technology and applications, in, Wiley Chichester, 2004.
[7] M.Y. Kariduraganavar, R.K. Nagarale, A.A. Kittur, S.S. Kulkarni, Ion-exchange membranes: preparative methods for electrodialysis and fuel cell applications, Desalination, 197 (2006) 225-246, https://doi.org/10.1016/j.desal.2006.01.019.
[8] H. Strathmann, Ion-exchange membrane separation processes, Elsevier, 2004.
[9] R.K. Nagarale, G.S. Gohil, V.K. Shahi, Recent developments on ion-exchange membranes and electro-membrane processes, Adv Colloid Interfac, 119 (2006) 97-130, https://doi.org/10.1016/j.cis.2005.09.005.
[10] B. Van der Bruggen, A. Koninckx, C. Vandecasteele, Separation of monovalent and divalent ions from aqueous solution by electrodialysis and nanofiltration, Water Res, 38 (2004) 1347-1353, https://doi.org/10.1016/j.watres.2003.11.008.
[11] C. Vallois, P. Sistat, S. Roualdes, G. Pourcelly, Separation of H^+/Cu^{2+} cations by electrodialysis using modified proton conducting membranes, J Membrane Sci, 216 (2003) 13-25, https://doi.org/10.1016/S0376-7388(03)00023-1.
[12] T. Sata, Studies on anion exchange membranes having permselectivity for specific anions in electrodialysis - effect of hydrophilicity of anion exchange membranes on permselectivity of anions, J Membrane Sci, 167 (2000) 1-31, https://doi.org/10.1016/S0376-7388(99)00277-X.
[13] T. Sata, K. Mine, M. Higa, Change in permselectivity between sulfate and chloride ions through anion exchange membrane with hydrophilicity of the membrane, J Membrane Sci, 141 (1998) 137-144, https://doi.org/10.1016/S0376-7388(97)00296-2.
[14] S. Abdu, M.C. Marti-Calatayud, J.E. Wong, M. Garcia-Gabaldon, M. Wessling, Layer-by-Layer Modification of Cation Exchange Membranes Controls Ion Selectivity and Water Splitting, Acs Appl Mater Inter, 6 (2014) 1843-1854, https://dx.doi.org/10.1021/am4048317.
[15] Y. Zhu, M. Ahmad, L. Yang, M. Misovich, A. Yaroshchuk, M.L. Bruening, Adsorption of polyelectrolyte multilayers imparts high monovalent/divalent cation selectivity to aliphatic polyamide

cation-exchange membranes, J Membrane Sci, 537 (2017) 177-185, https://doi.org/10.1016/j.memsci.2017.05.043.
[16] L.Y. Ng, A.W. Mohammad, C.P. Leo, N. Hilal, Polymeric membranes incorporated with metal/metal oxide nanoparticles: A comprehensive review, Desalination, 308 (2013) 15-33, https://doi.org/10.1016/j.desal.2010.11.033.
[17] T. Kikhavani, S.N. Ashrafizadeh, B. Van der Bruggen, Nitrate Selectivity and Transport Properties of a Novel Anion Exchange Membrane in Electrodialysis, Electrochim Acta, 144 (2014) 341-351, https://doi.org/10.1016/j.electacta.2014.08.012.
[18] S.M. Hosseini, M. Nemati, F. Jeddi, E. Salehi, A.R. Khodabakhshi, S.S. Madaeni, Fabrication of mixed matrix heterogeneous cation exchange membrane modified by titanium dioxide nanoparticles: Mono/bivalent ionic transport property in desalination, Desalination, 359 (2015) 167-175, https://doi.org/10.1016/j.desal.2014.12.043.
[19] C.H. Rhee, H.K. Kim, H. Chang, J.S. Lee, Nafion/sulfonated montmorillonite composite: A new concept electrolyte membrane for direct methanol fuel cells, Chem Mater, 17 (2005) 1691-1697, https://doi.org/10.1021/cm048058q.
[20] Y. Kim, J.S. Lee, C.H. Rhee, H.K. Kim, H. Chang, Montmorillonite functionalized with perfluorinated sulfonic acid for proton-conducting organic-inorganic composite membranes, J Power Sources, 162 (2006) 180-185, https://doi.org/10.1016/j.jpowsour.2006.07.041.
[21] S. Sasikala, S. Meenakshi, S.D. Bhat, A.K. Sahu, Functionalized Bentonite clay-sPEEK based composite membranes for direct methanol fuel cells, Electrochim Acta, 135 (2014) 232-241, https://doi.org/10.1016/j.electacta.2014.04.180.
[22] N. Kakati, J. Maiti, G. Das, S.H. Lee, Y.S. Yoon, An approach of balancing the ionic conductivity and mechanical properties of PVA based nanocomposite membrane for DMFC by various crosslinking agents with ionic liquid, Int J Hydrogen Energ, 40 (2015) 7114-7123, https://doi.org/10.1016/j.ijhydene.2015.04.004.
[23] M.M. Hasani-Sadrabadi, E. Dashtimoghadam, F.S. Majedi, K. Kabiri, Nafion (R)/bio-functionalized montmorillonite nanohybrids as novel polyelectrolyte membranes for direct methanol fuel cells, J Power Sources, 190 (2009) 318-321, https://doi.org/10.1016/j.jpowsour.2009.01.043.
[24] M. Namdari, T. Kikhavani, S.N. Ashrafizadeh, Synthesis and characterization of an enhanced heterogeneous cation exchange membrane via nanoclay, Ionics, 23 (2017) 1745-1758, https://doi.org/10.1007/s11581-017-2009-x.
[25] S.M. Hosseini, A. Seidypoor, M. Nemati, S.S. Madaeni, F. Parvizian, E. Salehi, Mixed matrix heterogeneous cation exchange membrane filled with clay nanoparticles: membranes' fabrication and characterization in desalination process, J Water Reuse Desal, 6 (2016) 290-300, https://doi.org/10.2166/wrd.2015.064
[26] G. Rytwo, A. Banin, S. Nir, Exchange reactions in the Ca-Mg-Na-montmorillonite system, Clays and Clay Minerals, 44 (1996) 276-285.
[27] G. Sposito, K.M. Holtzclaw, C. Jouany, L. Charlet, Cation selectivity in sodium-calcium, sodium-magnesium, and calcium-magnesium exchange on Wyoming bentonite at 298 K, Soil Science Society of America Journal, 47 (1983) 917-921, https://doi.org/10.2136/sssaj1983.03615995004700050015x.
[28] S.M. Hosseini, S.S. Madaeni, A.R. Khodabakhshi, Preparation and characterization of PC/SBR heterogeneous cation exchange membrane filled with carbon nano-tubes, J Membrane Sci, 362 (2010) 550-559, https://doi.org/10.1016/j.memsci.2010.07.015.
[29] C.E. Powell, G.G. Qiao, Polymeric CO_2/N_2 gas separation membranes for the capture of carbon dioxide from power plant flue gases, J Membrane Sci, 279 (2006) 1-49, https://doi.org/10.1016/j.memsci.2005.12.062.
[30] H. Farrokhzad, M.R. Moghbeli, T. Van Gerven, B. Van der Bruggen, Surface modification of composite ion exchange membranes by polyaniline, React Funct Polym, 86 (2015) 161-167, https://doi.org/10.1016/j.reactfunctpolym.2014.08.003.

[31] X. Li, Z. Wang, H. Lu, C. Zhao, H. Na, C. Zhao, Electrochemical properties of sulfonated PEEK used for ion exchange membranes, J Membrane Sci, 254 (2005) 147-155, https://doi.org/10.1016/j.memsci.2004.12.051.
[32] J. Schauer, L. Brozova, Heterogeneous ion-exchange membranes based on sulfonated poly (1,4-phenylene sulfide) and linear polyethylene: preparation, oxidation stability, methanol permeability and electrochemical properties, J Membrane Sci, 250 (2005) 151-157, https://doi.org/10.1016/j.memsci.2004.09.047.
[33] F.G. Wilhelm, I.G.M. Punt, N.F.A. van der Vegt, H. Strathmann, M. Wessling, Cation permeable membranes from blends of sulfonated poly(ether ether ketone) and poly(ether sulfone), J Membrane Sci, 199 (2002) 167-176, https://doi.org/10.1016/S0376-7388(01)00695-0.
[34] P. Dlugolecki, B. Anet, S.J. Metz, K. Nijmeijer, M. Wessling, Transport limitations in ion exchange membranes at low salt concentrations, J Membrane Sci, 346 (2010) 163-171, https://doi.org/10.1016/j.memsci.2009.09.033.
[35] C. Hannachi, B. Hamrouni, M. Dhahbi, Ion exchange equilibrium between cation exchange membranes and aqueous solutions of K^+/Na^+, K^+/Ca^{2+}, and Na^+/Ca^{2+}, Ionics, 15 (2009) 445-451, https://doi.org/10.1007/s11581-008-0292-2.
[36] H. Miyoshi, M. Yamagami, M. Chubachi, T. Kataoka, Characteristic Coefficients of Cation-Exchange Membranes for Bivalent-Cations in Equilibrium between the Membrane and Solution, J Chem Eng Data, 39 (1994) 595-598, Engineering Data, Vol.39, No.3, 595-598, 1994, https://doi.org/10.1021/je00015a045.
[37] L. Lazar, B. Bandrabur, R.E. Tataru-Farmus, M. Drobota, L. Bulgariu, G. Gutt, Ftir Analysis of Ion Exchange Resins with Application in Permanent Hard Water Softening, Environ Eng Manag J, 13 (2014) 2145-2152.
[38] Y.F. Lin, C.Y. Yen, C.H. Hung, Y.H. Hsiao, C.C.M. Ma, A novel composite membranes based on sulfonated montmorillonite modified Nafion for DMFCs, J Power Sources, 168 (2007) 162-166, https://doi.org/10.1016/j.jpowsour.2007.02.079.
[39] F. Parvizian, S.M. Hosseini, A.R. Hamidi, S.S. Madaeni, A.R. Moghadassi, Electrochemical characterization of mixed matrix nanocomposite ion exchange membrane modified by ZnO nanoparticles at different electrolyte conditions "pH/concentration", Journal of the Taiwan Institute of Chemical Engineers, 45 (2014) 2878-2887, https://doi.org/10.1016/j.jtice.2014.08.017.
[40] R. Förch, H. Schönherr, A.T.A. Jenkins, Surface design: applications in bioscience and nanotechnology, John Wiley & Sons, 2009.
[41] P. Daraei, S.S. Madaeni, N. Ghaemi, E. Salehi, M.A. Khadivi, R. Moradian, B. Astinchap, Novel polyethersulfone nanocomposite membrane prepared by PANI/Fe_3O_4 nanoparticles with enhanced performance for Cu(II) removal from water, J Membrane Sci, 415 (2012) 250-259, https://doi.org/10.1016/j.memsci.2012.05.007.
[42] S. Hosseini, S. Madaeni, A. Khodabakhshi, Preparation and characterization of ABS/HIPS heterogeneous anion exchange membrane filled with activated carbon, Journal of Applied Polymer Science, 118 (2010) 3371-3383, |https://doi.org/10.1002/app.32369.
[43] S.M. Hosseini, S.S. Madaeni, A.R. Heidari, A.R. Moghadassi, Preparation and characterization of polyvinyl chloride/styrene butadiene rubber blend heterogeneous cation exchange membrane modified by potassium perchlorate, Desalination, 279 (2011) 306-314, https://doi.org/10.1016/j.desal.2011.06.022.
[44] C. Fernandez-Gonzalez, B.P. Zhang, A. Dominguez-Ramos, R. Ibanez, A. Irabien, Y.S. Chen, Enhancing fouling resistance of polyethylene anion exchange membranes using carbon nanotubes and iron oxide nanoparticles, Desalination, 411 (2017) 19-27, https://doi.org/10.1016/j.desal.2017.02.007.
[45] G.M. Geise, M.A. Hickner, B.E. Logan, Ionic Resistance and Permselectivity Tradeoffs in Anion Exchange Membranes, Acs Appl Mater Inter, 5 (2013) 10294-10301, https://doi.org/10.1021/am403207w.
[46] T.W. Xu, Ion exchange membranes: State of their development and perspective, Journal of Membrane Science, 263 (2005) 1-29, https://doi.org/10.1016/j.memsci.2005.05.002.
[47] R.A. Horne, Marine Chemistry; the structure of water and the chemistry of the hydrosphere, (1969).

[48] T. Rijnaarts, E. Huerta, W. van Baak, K. Nijmeijer, Effect of divalent cations on RED performance and cation exchange membrane selection to enhance power densities, Environmental science & technology, 51 (2017) 13028-13035, https://doi.org/10.1021/acs.est.7b03858.

Graphical abstract